Treadmilling stability of a one-dimensional actin growth model

Rohan Ø. Abeyaratne[a], Eric Puntel[b,*], Giuseppe Tomassetti[c]

[a] *Department of Mechanical Engineering, Massachusetts Institute of Technology, Cambridge, MA, USA*
[b] *Dipartimento Politecnico di Ingegneria e Architettura, Università di Udine, via del Cotonificio 114, Udine I-33100, Italy*
[c] *Dipartimento di Ingegneria, Università degli Studi Roma Tre, via Volterra 62, Roma I-00146, Italy*

Abstract

Actin growth is a fundamental biophysical process and it is, at the same time, a prototypical example of diffusion-mediated surface growth. We formulate a coupled chemo-mechanical, one-dimensional growth model encompassing both material accretion and ablation. A solid bar composed of bound actin monomers is fixed at one end and connected to an elastic device at the other. This spring-like device could, for example, be the cantilever tip of an AFM. The compressive force applied by the spring on the bar increases as the solid grows and affects the rate of growth. The mechanical behaviour of the bar, the diffusion of free actin monomers in a surrounding solvent and the kinetic growth laws at the accreting/ablating ends are accounted for. The constitutive response of actin is model by a convex but otherwise arbitrary elastic strain energy density function. Treadmilling solutions, characterized by a constant length of the continuously evolving body, are investigated. Existence and stability results are condensed in the form of simple formulas and their physical implications are discussed.

Keywords: actin, treadmilling, stability, surface growth, Hookean spring

Here's a thought for the discussion section: The positions of the two tips of the bar in physical space are $y_1(t)$ and Y_0 and so the velocity of the moving tip is $\dot{y}_1$. By differentiating $y_1(t) - Y_0 = \widehat{\lambda}(\sigma(t))\ell(t)$ with respect to t one can show that

$$\dot{y}_1 = \frac{\widehat{\lambda}^2(\sigma)}{\widehat{\lambda}(\sigma) + (\sigma_{\max} - \sigma)\widehat{\lambda}'(\sigma)} [R_1(\sigma) - R_0(\sigma)].$$

Is it worth plotting $\dot{y}_1$ versus $|\sigma|$ from some initial stress until treadmilling? This might be like the F-v curve in the Fletcher group papers (Parekh, Chaudhuri

*Corresponding Author.
Email addresses: rohan@mit.edu (Rohan Ø. Abeyaratne), eric.puntel@uniud.it (Eric Puntel), giuseppe.tomassetti@uniroma3.it (Giuseppe Tomassetti)

& Bieling) with treadmilling being what they call stall. Just a thought. Less important if we are sending to an Applied Math journal, but might be worth considering for a Solid Mechanics journal.

sec:intro

1. Introduction

It is well known that growth in living systems is not only promoted by biological and chemical signals but is also affected by mechanical stimuli (**?**).

Modelling growth, intended as variation of mass, poses a number of challenges in mechanics which are still being actively investigated. Among them is surface growth or accretion which, following the work of Skalak and others (**??**), requires one to define and track in time an ever changing, usually stress-free, reference configuration, i.e. collection of material points. The phenomenon of accretion of a solid on its boundary, occurs in several contexts of physical, technological, and biological interest. One of the most common examples of surface growth is the solidification of water at the ice-water interface near the freezing temperature; other examples include technological processes such as chemical vapor deposition, 3D printing and layered building (**???**); in biology, the growth of hard tissues like bones and teeth (**??**). When surface growth occurs at an interior surface it generates stress, since each new layer of solid material that forms must push away the layers deposited previously.

A second delicate issue regards the prescription of a growth law. One may simply assume that as given. Conversely, growth speed could be obtained as a result of mechanical and biochemical local conditions. These in turn may be expressed by a suitable kinetic law once the thermodynamical force driving growth has been consistently defined (**??**).

Third, one may also describe the transport of the free particles that provide the material constituents for growth. In this way essential features of growth may emerge from the balance of coupled mechanical and biochemical responses.

In this work we formulate and analyze a one-dimensional model featuring the three aforementioned characteristics, albeit in a simplified manner. We consider an elastic bar fixed at one end and connected to an elastic device at the other. This spring-like elastic device could for example be the cantilever tip of an atomic force microscope as in the experiments described in (**???**). The bar can grow by attaching or detaching its constituting particles ("monomers"), at either end. The diffusion of free particles in a surrounding or permeating solvent and the kinetic condition for growth are accounted for. The first objective of this study is to investigate a basic reference template of chemo-mechanical growth which allows one to discuss more easily modelling choices, notions and solutions.

The second motivation for this study is provided by a specific biological example, namely the growth of actin filaments. Actin in its polymerized network-forming state is an essential constituent of the cytoskeleton and is involved in cell contraction, division and motility. It is intensely studied in the bio-physical literature. See e.g. **?** for a review on the physics of active gels like actin, the Ph.D. thesis of **?** for a review of quantitative models of actin-based motility,

and **?** and **?** for just two of the many examples of different biophysical and computational models of the properties of actin networks. Pertinent to this study, but not including mechanical aspects, is a one-dimensional mathematical model of actin polymerization kinetics by **?**.

Of particular interest are the experimental studies described in **??** and **?** that involve an experimental setup similar to the one considered here, where an actin network is grown between the cantilever tip of an atomic force microscope (AFM) and a fixed surface below it thus realizing a bar-like structure fixed at one end and restrained by an elastic device at the other. Among other things, these experiments consistently suggest that the actin network adapts to higher values of applied compressive force by correspondingly increasing its density and stiffness. This is a feature that is currently not included in our model, but it constitutes a possible refinement for future work. My reading of some of these papers is not that the stiffness changes directly because of growth. More that the constitutive function $\widehat{\sigma}(\lambda) = W'(\lambda)$ changes its curvature as λ increases. The increase in λ maybe due to growth but I didn't think they were suggesting that $W(\lambda, growth)$. I could be wrong. I suggest we drop stiffness but keep density.

Actin filaments exhibit a peculiar growth mode called treadmilling in which the length of the filament in physical space remains constant while accreting (i.e. attaching) actin monomers at one end and ablating (i.e. detaching) them at the other at equal rates (see e.g. **?**). This energy dissipating state is made possible by the energy provided by the hydrolysis of the ATP (adenosine triphosphate) bound to actin monomers into an ADP (adenosine diphosphate) molecule and a phosphate. Despite its peculiarity, treadmilling may also be seen as a specific instance of a more common biological paradigm by which systems, tissues or organisms continuously substitute their constituents or cells at specific rates even when their overall size is no longer changing.

The present work has two main results. First, under rather general assumptions on the behaviour of the material constituting the bar, we establish conditions for the existence of treadmilling states in terms of simple formulas.

Second, the stability of such solutions is discussed. Herein stability is not addressed energetically in classical structural mechanics terms (i.e. buckling) by considering perturbations perpendicular to the bar but rather dynamically, asking whether perturbations in the direction of the bar of the treadmilling state may cause the bar to abandon indefinitely its stationary length. For the treadmilling case in which ATP is attached to the actin molecules accreting at the fixed end of the bar, it is possible to prove global stability under arbitrary initial conditions.

These results pertaining to the existence, uniqueness and stability of treadmilling states is discussed in physical terms in the last section of this paper.

We expect that the present results will be useful tool in the ~~can hopefully~~ comparison and interpretation of other more complex models and experiments. For instance, our results on the global stability of a treadmilling solution may provide clarification or further evidence in support of the "emergence of a universal growth path" observed in a roughly similar context by **?**.

The discussion on stability of the solution has also been motivated by experiments studying the growth and relative stability of an annulus of actin accreting on the surface of a spherical bead (**???**). These experiments were in turn inspired by bacterium Listeria monocytogenes which exploits cytoplasmic actin to form a polymerized tail and move out of the cell membrane and spread (**?**). Existing numerical and modelling efforts on this subject can be found in (**??**).

A model for a spherical annulus of actin growing on the surface of a sphere was formulated and analyzed by **?**. Treadmilling solutions were studied there as well but not their stability. We plan to continue the above study and the present one by the analysis of the stability of the treadmilling solutions of that spherical annular system. Other extension of the present work include accounting for the aforementioned dependence of actin see previous remark about stiffness ~~stiffness~~ and density on externally applied stress and deriving analytical relationships between growth velocity and external force to be compared with experimental ones.

This paper is structured as follows. Section 2 describes the one-dimensional model including its mechanical, chemical and growth aspects. Section 3 provides the material constitutive description of the bar while the derivation of the driving force is given in Section 4. The system is reduced to a differential algebraic equation in Section 5, a form that is particularly suitable for the subsequent discussion of the existence, uniqueness and stability of treadmilling solutions that is carried out in Section 6. The results are discussed and concluding remarks are made in Section 7.

sec:model

2. One-dimensional model

ss:set

2.1. Problem setting

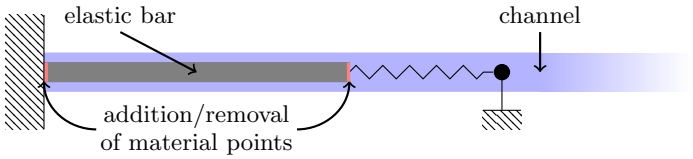

Figure 1: An elastic bar clamped between a hard and a soft device, immersed in a semi-infinite channel.

fig:setup

We consider a one-dimensional body, represented by a bar in Figure 1, which grows and deforms in a one-dimensional physical space.

The bar has a natural reference configuration that occupies the segment $(x_0(t), x_1(t))$ and whose generic point is denoted by x . Here and in the following subscripts 0 and 1 refer to the left and right end sections of the bar respectively, both in the reference and in the current configurations.

As represented in Figure 2, the body is mapped into (?) the physical one-dimensional space through the function $y(x,t)$ where it occupies the segment

$(y_0(t), y_1(t))$. Here and in what follows the shorthand notation

$$f_\alpha(t) = f(x_\alpha(t), t) \qquad \text{with } \alpha = 0, 1\ , \tag{1}$$

eq:fam

denotes in general the value of a material quantity $f(x,t)$ at the end sections of the bar at time t. In particular $y_0(t)$ and $y_1(t)$ simply indicate the position of the end sections of the bar in the current configuration.

In your previous version of Fig 2 you had $x_0(t), x_1(t)$ and $y_1(t)$ but you've removed the "t"s now (except in $y(x,t)$. Was there a reason for removing the "t"s??

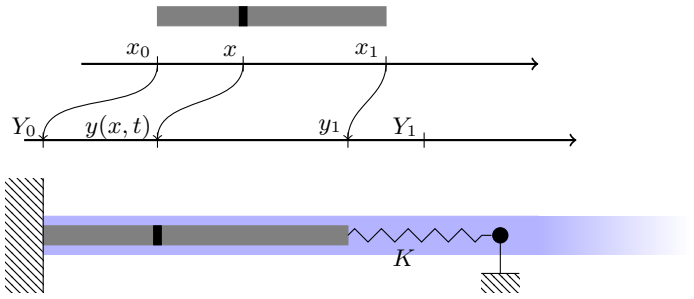

Figure 2: Reference (top) and current (bottom) configuration of the elastic bar.

fig:onedim

In regard to constraints, the terminal side x_0 of the bar is attached to the point Y_0 in the physical space, so that $y_0 = y(x_0(t), t) = Y_0$. Likewise, the terminal side x_1 is attached to one end of a linear spring of stiffness K. The rest position of this end of the spring is Y_1, i.e. the spring is unstretched with zero force when this end is at Y_1. Its other end is fixed. It is worth noting that while the left-hand end of the bar is always located at Y_0 in physical space, the right-hand end is located at Y_1 only when the spring force vanishes.

The bar is made of "material units", hereafter referred to as *monomers*, which are in a bound, polymerized state. The same monomers in a free, unbound state are in solution in the solvent which fills a one dimensional infinite channel, depicted with a blue-shaded rectangle in Figure 1. Free monomers flow in the interval $(y_0(t), y_1(t)) = (Y_0, y_1(t))$ according to Fick's law. We can think of them as either flowing only through the bar or flowing as well through the portion of the channel not occupied by the bar. They can freely cross the point y_1, where the body is in contact with a reservoir of monomers, but cannot flow past the left support $y_0 = Y_0$ which is assumed to be impermeable. The chemical potential μ_1 of free monomers at $y_1(t)$ is held fixed and equal to M_1 , and there is an infinite supply of monomers at y_1.

I tried consistently using capital letters Y,M for prescribed values, small case for fields y,μ, and subscripts y_α,μ_α for values of the fields at the end cross sections.

Finally, under suitable growth conditions to be later specified, free monomers may accrete, i.e. attach, at either end of the bar and conversely, bound monomers occupying the end positions x_0 and x_1 of the bar may ablate, i.e. detach, and return to their free state. When accretion or ablation occurs, the referential points x_0 and x_1, and hence the reference length of the bar, can change. Specifically, at the left-hand end x_0, accretion occurs when $\dot{x}_0 < 0$ while ablation occurs when $\dot{x}_0 > 0$. Similarly accretion and ablation at the right-hand end x_1 correspond to $\dot{x}_1 > 0$ and $\dot{x}_1 < 0$ respectively.

We now specify the equations governing the system just described.

ss:mech

2.2. *Mechanics*

We require the deformation mapping $y(x,t) : x \to y$ to be one to one by prescribing that the stretch $\lambda = y' = \partial y/\partial x$ be positive:

$$\lambda(x,t) = y'(x,t) > 0 \, .$$

Here and in the following we use the prime to denote the derivative with respect to a variable other than time. That is $f' = \partial f/\partial \bullet$ with $f = f(\bullet)$ or $f = f(\bullet, t)$ with t indicating time and $\bullet \neq t$. The dot is used, as customary, to indicate partial derivative with respect to time, i.e. $\dot{f} = \partial f/\partial t$.

We assume the material to be hyperelastic and therefore characterized by a convex strain energy density $W(\lambda)$ from which we can compute the axial force σ in the bar as

$$\sigma(x,t) = W'(\lambda(x,t)) \, .$$

A number of additional assumptions on the strain energy density are detailed in Section 3.1. Given that W does not depend explicitly on x, the material constituting the bar is taken to be homogeneous.

eq:mech

The mechanical model for the bar is summarized in the set of equations (2) below.

$$\begin{cases} \dfrac{\partial \sigma}{\partial x} = 0 & \text{in } (x_0(t), x_1(t)), \quad (2a) \quad \texttt{eq:mech1} \\ \sigma = W'(\lambda), \quad \lambda = y' & \text{in } (x_0(t), x_1(t)), \quad (2b) \quad \texttt{eq:mech2} \\ y_0(t) = y(x_0(t), t) = Y_0 & \text{in } x_0(t), \quad (2c) \quad \texttt{eq:mech3} \\ \sigma_1(t) + K(y_1(t) - Y_1) = 0 & \text{in } x_1(t) \, . \quad (2d) \quad \texttt{eq:mech4} \end{cases}$$

Equation (2a) represents local equilibrium in the reference configuration and implies that the axial force is constant in x. In eq. (2b) we state again the constitutive law and the definition of the stretch λ. Being σ constant in x, it follows that λ is constant in x and that y is linear in x.

The boundary condition prescribing that the leftmost section of the bar is fixed in $y = Y_0$ is expressed in eq. (2c). The axial force $\sigma_1(t) = \sigma(x_1(t), t)$ in the bar at $x = x_1(t)$ is prescribed by the force in the spring of stiffness K in eq. (2d). Since σ is independent of x, (2d) actually prescribes the value of the axial force in the whole bar.

ss:diff

2.3. *Diffusion*

eq:diff

The following system

$$\begin{cases} \dfrac{\partial h}{\partial y} = 0 & \text{in } (Y_0, y_1(t)), \quad (3a) \quad \texttt{eq:diff1} \\ h + m\mu' = 0 & \text{in } (Y_0, y_1(t)), \quad (3b) \quad \texttt{eq:diff2} \\ h(y_0(t), t) = h(Y_0, t) = \varrho \dot{x}_0(t) & \text{in } Y_0, \quad (3c) \quad \texttt{eq:diff3} \\ \mu(y_1(t), t) = M_1 & \text{in } y_1(t) \, . \quad (3d) \quad \texttt{eq:diff4} \end{cases}$$

governs the flux of free monomers in the solvent. Here $h(y,t)$ is the monomer flux in the positive y direction, $\mu(y,t)$ is the associated chemical potential and m is the mobility. The first equation (3a) expresses the conservation of mass. In it we have omitted a term $\partial h/\partial t$ by assuming that diffusion is much faster than growth. Flux has the dimension of moles per unit time. The second equation (3b) represents Fick's law. The third equation (3c), a boundary balance of mass, states that the flux of monomers at the impermeable wall is equal to the amount of monomers that detach from the left endpoint of the bar per unit time, which in turn is proportional to the ablation velocity $\dot{x}_0$ through a constant ϱ. We think of ϱ as the number of moles of bound actin monomer per unit length in the reference configuration. The fourth equation (3d) expresses the condition of chemical equilibrium at y_1 by equating $\mu_1 = \mu(y_1(t),t)$ to the chemical potential M_1 of the monomers in the semi-infinite monomer pool to the right of y_1. Note that $\mu_0 = \mu(y_0,t)$ is as yet unknown and to be determined.

We could use the prime in (2a) and (3a) if you prefer. I did not use it because I wanted to highlight the dependence on x and y respectively.

If we use μ_0 for $\mu(y_0,t)$, I am uncomfortable using μ_1 for both $\mu(y_1,t)$ and M_1. Should we extend the notation def. in eq. (1)?

ss:accr

2.4. Accretion

As anticipated in the Introduction, a key ingredient of this model is the growth law governing the evolution of the referential configuration of the bar. We assume a simple, linear kinetic law of the form

$$B_\alpha V_\alpha = F_\alpha \qquad \text{with } \alpha = 0,1 \tag{4}$$

eq:kinshort

In eq. (4), $\alpha = 0,1$ refer to the ends of the bar, V_α is the accretion velocity, B_α is a positive kinetic coefficient and F_α is the thermodynamical force driving accretion. Note that $V_0 = -\dot{x}_0$ and $V_1 = \dot{x}_1$. Realistically (4) is most suitable for small deviations from thermodynamic equilibrium. The expression for F_α, derived afterwards in Section 4, is

$$F_\alpha = \varrho(\mu_\alpha - M_{B,\alpha}) + W^*(\sigma_\alpha), \tag{5}$$

eq:Fa

where σ_α and μ_α are *material* descriptions of the fields μ, σ evaluated at x_α following the notation introduced in (1). Parameter $M_{B,\alpha}$ is a material constant interpreted as the chemical potential of *bound* monomers at x_α and $W^*(\sigma)$ is the *complementary* strain energy density whose definition and properties are given in Section 3.2. In particular in there we will see that a tensile force $\sigma > 0$ corresponds to positive $W^*(\sigma)$ thus promoting growth according to (4)-(5). This is consistent with the layman's notion of stress induced growth popularized by images of abnormal growth of earlobes, necks and other body parts subject to sustained tension, especially observed in some indigenous tribes (see e.g. **?**, Chapter 2.1).

Motivated by the behaviour of actin filaments, see e.g. **?** or **?**, panel 16-2, we admit two distinct values $M_{B,0}$ and $M_{B,1}$ for the chemical potential of monomers in the bound state. Actin monomers are bound to ATP (Adenosine TriPhosphate) when they first polymerize, i.e. accrete, but after some time a hydrolysis reaction ensues by which the ATP releases a phosphate group and the polymerized actin monomer is now tied to an ADP (Adenosine DiPhosphate)

molecule. The hydrolysis reaction releases energy, part of which remains stored in the polymerized actin (Rohan's comment: I don't understand this. On one hand it is released, on the other it is stored? ⟶ see **?**, page 901). Therefore ADP-actin is at a higher energy level, i.e. chemical potential, than ATP-actin. Due to differences in the properties of opposite ends of actin filaments, one end may be occupied by a lower-energy ATP-actin monomer and the other by a higher energy ADP bound actin monomer. Hence the distinction between values of the chemical potential of polymerized actin $M_{B,0}$ and $M_{B,1}$ at the two ends of the bar.

removed, "barbed" and "pointed", but not added inequality $M_{B,0}$ smaller than $M_{B,1}$

As noted previously, a positive accretion velocity corresponds to a negative rate $\dot{x}_0$ and to a positive rate $\dot{x}_1$ whence $V_0 = -\dot{x}_0$ and $V_1 = \dot{x}_1$, and recalling that we are using the notation of equation (1), the specialization of (4) and (5) to the two ends of the bar can be written as

eq:accr

$$\begin{cases} -B_0\dot{x}_0(t) = \varrho(\mu_0 - M_{B,0}) + W^*(\sigma_0(t)) \,, & \text{(6a)} \\ \quad B_1\dot{x}_1(t) = \varrho(\mu_1 - M_{B,1}) + W^*(\sigma_1(t)) \,. & \text{(6b)} \end{cases}$$

eq:accr1 eq:accr2

Since you have stated this inequality in words in the text, is it helpful to display it as well?

Despite the simplicity of the one-dimensional model, the above equations close the feedback loop between stress and growth. On the one hand, the presence of the spring in (2) allows growth to affect stress, while on the other hand, growth rates in (6) are influenced by stress.

The evolution equations (6) also provide closure for the boundary-value problem (2) and (3). In fact, the solution of (2)–(3) depends only on the instantaneous values of $x_0(t)$, $x_1(t)$ and of the rate $\dot{x}_0(t)$. This means, in particular, that the right-hand sides of the equations (6) ultimately depend only on $x_0(t)$, $x_1(t)$ and $\dot{x}_0(t)$. We therefore conclude that the combination of (2), (3), and (6) is equivalent to a first-order system in the unknowns $x_0(t)$ and $x_1(t)$. As such, this system must be complemented by initial conditions

$$x_0(0) = x_{00}, \qquad x_1(0) = x_{10} \quad \text{and} \quad y_0(0) = Y_{00} = Y_0, \qquad y_1(0) = Y_{10}. \quad (7)$$

eq:xyinit

I think you can only give x_{10} and x_{00} since Y_{10} is then determined. From $(25)_1$ and (7)

$$\lambda(0) \overset{(25)_1,(7)}{=} \frac{Y_{10} - Y_0}{x_{10} - x_{00}} \qquad (*)$$

From $(25)_2$ and (22c)

$$\sigma(0) \overset{(25),(22c)}{=} \sigma_{max} - K(Y_{10} - Y_0) \qquad (**)$$

Using $(*)$ and $(**)$ in

$$\sigma(0) = \widehat{\sigma}(\lambda(0))$$

relates x_{10}, x_{00} and Y_{10}.

I suggest giving Y_{10} which is a physical space boundary condition, and either x_{10} or x_{00}. If $x_0(t), x_1(t)$ is a solution then so is $x_0(t) + c, x_1(t) + c$ for any constant c. So this one initial condition on $x_0(t)$ (or $x_1(t)$) is just a matter of

picking a datum for the reference space. For example if $y_1(0) = Y_1$ and no other initial conditions are given, you find $\sigma(0) = 0, \lambda(0) = 1, \ell(0) = Y_1 - Y_0$ etc. so you see that x_{10} is really not important, but it has to be given of course if we want to find $x_1(t)$ and $x_0(t)$.

sec:const

3. Constitutive behaviour

We assume the bar to be made of a homogeneous, hyperelastic material and we define its constitutive behaviour through the strain energy density function $W(\lambda)$. As seen in equation (2b), the force σ is given by $W'(\lambda)$ while $W''(\lambda)$ represents the tangent stiffness.

ss:W

3.1. Strain energy density

A specific expression for $W(\lambda)$ is not prescribed. Instead, we merely assume that the strain energy density has the following characteristics:

eq:Wass

$$\begin{cases} W(1) = 0 & & \text{(8a)} \quad \texttt{eq:Wass1} \\ W'(1) = 0 & & \text{(8b)} \quad \texttt{eq:Wass2} \\ W(\lambda) \to +\infty & \text{as } \lambda \to 0^+ & \text{(8c)} \quad \texttt{eq:Wass3} \\ W(\lambda) \to +\infty & \text{as } \lambda \to +\infty & \text{(8d)} \quad \texttt{eq:Wass4} \\ W'(\lambda) \to +\infty & \text{as } \lambda \to +\infty & \text{(8e)} \quad \texttt{eq:Wass5} \\ W''(\lambda) > 0 & \forall \lambda > 0 & \text{(8f)} \quad \texttt{eq:Wass6} \end{cases}$$

discussed in the following.

The strain energy density is defined but for an arbitrary constant which is conveniently set in (8a) by assigning zero energy to the undeformed state in which the stretch λ is equal to 1. In this latter case the force σ is also zero according to eq. (8b). Equations (8c) and (8d) express the requirement that infinite strain energy is necessary to, respectively, infinitely compress and infinitely extend the material. Probably the strongest condition on $W(\lambda)$ is given by eq. (8f) which enforces convexity of the strain energy which in turn implies that the stress is a monotonic function of the stretch, and the tangent stiffness is positive everywhere, i.e. there are no stress softening branches under increasing stretch. Note that $\sigma > 0$ for $\lambda > 1$ and $\sigma < 0$ for $0 < \lambda < 1$. Assuming sufficient regularity of $W(\lambda)$, equations (8c) and (8f) can be used to prove that, when the stretch tends to zero, the force tends to infinity, that is $\sigma \to -\infty$ when $\lambda \to 0^+$. It is easy to see that conditions (8d) and (8f) are not sufficient to obtain an analogous result for the case in which the stretch tends to infinity. The condition that $\sigma \to +\infty$ when $\lambda \to +\infty$ is therefore explicitly given in (8e). We note in passing that the set of assumptions (8) is introduced in a constructive way and is not minimal since (8d) follows from (8e) and (8f).

From the properties of $W(\lambda)$ ensue those of the force σ. Let

$$\widehat{\sigma}(\lambda) := W'(\lambda) \quad , \quad \widehat{\sigma}(\lambda) : \mathbb{R}^+ \longrightarrow \mathbb{R} \, . \qquad (9) \quad \texttt{eq:shat}$$

Then from (8f) we know that $\widehat{\sigma}$ is monotonically increasing and, taking into account (8c)-(8e) as well, that it spans the whole real line.

The force $\widehat{\sigma}$ as a function of the stretch is therefore invertible and function

$$\widehat{\lambda}(\sigma) : \mathbb{R} \longrightarrow \mathbb{R}^+ , \quad \widehat{\lambda}(\sigma) \text{ such that } W'(\widehat{\lambda}) = \sigma \tag{10}$$ eq:lhat

is uniquely defined. It can be easily seen that $\widehat{\lambda}(\sigma)$ is monotonically increasing

$$\widehat{\lambda}'(\sigma) = \frac{1}{W''(\lambda)} > 0 \tag{11}$$ eq:lhat'

and that it possesses the following properties:

$$\widehat{\lambda}(\sigma) \to 0^+ \text{ as } \sigma \to -\infty, \qquad \widehat{\lambda}(0) = 1, \qquad \widehat{\lambda}(\sigma) \to +\infty \text{ as } \sigma \to +\infty. \tag{12}$$ eq:lhatprop

ss:W*

3.2. Complementary strain energy density

The complementary strain energy density $W^*(\sigma)$ is the Legendre transform of $W(\lambda)$. It defined as

$$W^*(\sigma) = \sigma\widehat{\lambda}(\sigma) - W(\widehat{\lambda}(\sigma)) , \tag{13}$$ eq:W*def

eq:W*

and has the properties

$$\begin{cases} W^{*\prime}(\sigma) = \lambda > 0 & \text{with } \lambda = \widehat{\lambda}(\sigma) \quad (14a) \quad \texttt{eq:W*1} \\ W^{*\prime\prime}(\sigma) = \widehat{\lambda}'(\sigma) > 0 & \forall \sigma \in \mathbb{R} \quad (14b) \quad \texttt{eq:W*2} \\ W^{*\prime}(\sigma) \to 0^+ & \text{as } \sigma \to -\infty \quad (14c) \quad \texttt{eq:W*3} \\ W^{*\prime}(\sigma) \to +\infty & \text{as } \sigma \to +\infty \quad (14d) \quad \texttt{eq:W*4} \\ W^*(0) = 0 & \quad (14e) \quad \texttt{eq:W*5} \\ W^*(\sigma) \to \pm\infty & \text{as } \sigma \to \pm\infty \quad (14f) \quad \texttt{eq:W*6} \end{cases}$$

all of which follow from assumptions we have made previously. The key property of $W^*(\sigma)$ is (14a). It ensues from the definition (13) since

$$W^{*\prime}(\sigma) = \widehat{\lambda}(\sigma) + \sigma\widehat{\lambda}'(\sigma) - W'(\lambda)\widehat{\lambda}'(\sigma) = \widehat{\lambda}(\sigma) .$$

Given that λ is always positive, we have that $W^*(\sigma)$ is a monotonically increasing function. Moreover, (14b) follows from (11) whence $W^*(\sigma)$ is also strictly convex. Properties (14c) and (14d) are simply restatements of (12). Property (14e) follows from the definition of $W^*(\sigma)$ and, together with monotonicity, implies that $W^*(\sigma) > 0$ when $\sigma > 0$ and $W^*(\sigma) < 0$ when $\sigma < 0$. The last property (14f) follows as well from the definition and the preceding properties. It is important because it implies that $W^*(\sigma) : \mathbb{R} \longrightarrow \mathbb{R}$ is surjective, and given the injectivity implied by (14a), also invertible. We will use this result in what follows, so it is worth noticing that it is a consequence of the assumptions (8c) and (8e).

ss:Wex

3.3. *Examples of strain energy density functions*

Consider moving this to an appendix. We provide here a couple of examples of strain energy density functions satisfying the requirements in eq. (8). We add also some remarks on the asymptotic growth of the constitutive laws $\widehat{\sigma}(\lambda)$ for stress and $W^*(\sigma)$ for the complementary strain energy density function ensuing from the choices of the asymptotic dominant term of the strain energy density W.

Adding the examples in order to use them for figures

Example 1: A rational function

First consider the rational strain energy density

$$W(\lambda) = \frac{EA}{6}(\lambda^2 + 2\lambda^{-1} - 3)\,, \tag{15}$$

eq:Wex1

where $EA > 0$ is a constant. It follows that $\sigma = W'(\lambda) = \frac{EA}{3}(\lambda - \lambda^{-2}), W''(\lambda) = \frac{EA}{3}(1 + 2\lambda^{-3}) > 0$ and $W''(1) = EA$. Notice that this W obeys all assumptions in (8). Then the complementary energy W^* can be obtained,

$$W^* = \frac{EA}{6}\left[\lambda^2 - 4\lambda^{-1} + 3\right]\Big|_{\lambda=\widehat{\lambda}(\sigma)}\,,$$

together with its derivatives,

$$W^{*\prime}(\sigma) = \lambda\Big|_{\lambda=\widehat{\lambda}(\sigma)} > 0 \quad \text{and} \quad W^{*\prime\prime}(\sigma) = \frac{3}{EA(1+2\lambda^{-3})}\Big|_{\lambda=\widehat{\lambda}(\sigma)} > 0\,.$$

The closed form expression of W^* is cumbersome, but we can easily look at its asymptotic behaviour when $\sigma \to \pm\infty$add colon to end of the preceding sentence. Note minus sign below.

$$W^* \sim \frac{3}{2}\frac{\sigma^2}{EA} \to +\infty \quad \text{for } \sigma \to +\infty, \qquad W^* \sim -\sqrt{\frac{4}{3}EA}\,\sqrt{-\sigma} \to -\infty \quad \text{for } \sigma \to -\infty$$

More generally, suppose that

$$W(\lambda) \sim \alpha\lambda^n, \qquad \sigma \sim \alpha n\lambda^{n-1}, \qquad \alpha > 0, n > 1, \qquad \text{as } \lambda \to \infty.$$

Then

$$\lambda \sim \left(\frac{\sigma}{\alpha n}\right)^{\frac{1}{n-1}}, \qquad W^* \sim \alpha(n-1)\left(\frac{\sigma}{\alpha n}\right)^{\frac{n}{n-1}} \to +\infty \qquad \text{as } \sigma \to +\infty.$$

Similarly suppose

$$W(\lambda) \sim \beta\lambda^{-m}, \qquad \sigma \sim -\beta m\lambda^{-m-1}, \qquad \beta > 0, m > 0, \qquad \text{as } \lambda \to 0.$$

Then

$$\lambda \sim \left(\frac{\beta m}{-\sigma}\right)^{\frac{1}{m+1}}, \qquad W^* \sim -\beta(m+1)\left(\frac{-\sigma}{\beta m}\right)^{\frac{m}{m+1}} \to -\infty \qquad \text{as } \sigma \to -\infty$$

Example 2: A closed form expression

A second example of a suitable strain energy density ~~of the form~~ is

$$W(\lambda) = \frac{EA}{2}\left(\frac{\lambda^2}{2} - \ln\lambda - \frac{1}{2}\right), \qquad \sigma = W'(\lambda) = \frac{EA}{2}\left(\lambda - \lambda^{-1}\right) \quad \textit{add comma}$$

where $EA > 0$ is a constant. Associated with this W one has, in closed form,

$$\widehat{\lambda}(\sigma) = \frac{\sigma}{EA} + \sqrt{\frac{\sigma^2}{(EA)^2} + 1}\,; \quad W^*(\sigma) = \frac{EA}{2}\left(\frac{\widehat{\lambda}^2(\sigma)}{2} + \ln\widehat{\lambda}(\sigma) - \frac{1}{2}\right). \tag{16}$$

eq:W*ex2

Also in this case we have that $W''(1) = EA$ and one can readily verify that W satisfies all requirements in (8).

sec:kinder

4. Derivation of the driving force

Accretion is a non-equilibrium process involving dissipation. The latter can be computed as the product of a flux, accretion rates in our case, and of a conjugate driving force which quantifies the departure from thermodynamic equilibrium.

In this section we provide the derivation of the expression of the driving force in eq. (5). We follow **?** and **??**.

We start from the expression of the dissipation rate associated with the bar,

$$\text{dissipation rate} \coloneqq \sigma\frac{dy}{dt}\Big|_{x_0}^{x_1} + \varrho(\mu - M_B)\dot{x}\Big|_{x_0}^{x_1} - \frac{d}{dt}\int_{x_0}^{x_1} W(\lambda)dx\,, \tag{17}$$

eq:dissdef

which is given by the sum of three terms. The first represents the mechanical power of external loads, the second the inflow of chemical energy per unit time and the third the energy flow per unit time elastically stored in the material and therefore not dissipated.

We observe that the velocity of a point on the boundary is given by

$$\dot{y}_\alpha(t) = \frac{d}{dt}y(x_\alpha(t), t) = v_\alpha + y'\dot{x}_\alpha = v_\alpha + \lambda_\alpha\dot{x}_\alpha, \tag{18}$$

eq:vel

from which we see that it is distinct from the velocity v_α of a material point sitting at the boundary at the current instant; here $v_\alpha(t) = v(x_\alpha(t), t)$ where $v(x,t) = \partial y(x,t)/\partial t$.

We rewrite the third term in (17) using Leibnitz's rule (the divergence theorem in one-dimension), transport theorems and equations (2a) and (2b),

$$\begin{aligned}\frac{d}{dt}\int_{x_0}^{x_1} W(\lambda)dx &= \int_{x_0}^{x_1} W'(\lambda)(\dot{y})'dx + W(\lambda)\dot{x}\Big|_{x_0}^{x_1} \\ &= (\sigma\dot{y} + W(\lambda))\dot{x}\Big|_{x_0}^{x_1}.\end{aligned} \tag{19}$$

eq:Wdiv

On substituting equations (18) and (19) into the expression (17) of the dissipation rate we obtain

$$\begin{aligned}\text{dissipation rate} &= (\sigma\dot{y} + \sigma\lambda\dot{x} + \varrho(\mu - M_B)\dot{x} - (\sigma\dot{y} + W(\lambda))\dot{x})\Big|_{x_0}^{x_1} \\ &= (\varrho(\mu - M_B) + (\sigma\lambda - W(\lambda)))\,\dot{x}\Big|_{x_0}^{x_1} \qquad (20) \quad \texttt{eq:diss2} \\ &= \Big(\varrho(\mu - M_B) + W^*(\sigma)\Big)\dot{x}\Big|_{x_0}^{x_1},\end{aligned}$$

in which the multiplier of the accretive flux $\dot{x}$ is precisely the driving force of growth introduced in equation (5).

sec:DAE

5. Reduction to a differential algebraic equation

Here the system of equations presented in Section 2 is reduced to a differential algebraic equation and new notation is introduced, suitable for the ensuing discussion on the existence and stability of treadmilling solutions.

ss:DAEmech

5.1. Mechanics

Let

$$\ell(t) = x_1(t) - x_0(t) > 0\,, \qquad (21) \quad \texttt{eq:ell}$$

be the length of the bar in the reference configuration. The integration of the mechanical system of equations (2) yields

eq:msol

$$\begin{cases} y(x,t) = \lambda(t)(x - x_0(t)) + Y_0, & \forall\ x_0(t) \le x \le x_1(t) \qquad (22a) \quad \texttt{eq:msol1} \\ \sigma(t) = W'(\lambda(t)) \qquad (22b) \quad \texttt{eq:msol2} \\ K\lambda(t)\ell(t) = \sigma_{\max} - \sigma(t) \qquad (22c) \quad \texttt{eq:msol3} \end{cases}$$

where we have termed

$$\sigma_{\max} = K(Y_1 - Y_0) \qquad (23) \quad \texttt{eq:smaxdef}$$

the maximum force attainable in the bar and in the spring. Since both $\lambda > 0$ and $\ell > 0$, it follows from (22c) that

$$\sigma < \sigma_{\max}. \qquad (24) \quad \texttt{eq:s<smax}$$

We consider $\sigma_{\max}$ to be an arbitrarily tunable parameter since we can imagine being able to vary the rest position Y_1 of the spring, to the right or to the left of Y_0, to attain any desired value of $\sigma_{\max}$.

From (22a) we have

$$\lambda = (y_1 - y_0)/(x_1 - x_0) = (y_1 - y_0)/\ell \qquad \Rightarrow \qquad (y_1 - y_0) = \lambda\ell \qquad (25) \quad \texttt{eq:lamell}$$

and so, as expected, $\lambda\ell$ denotes the length of the body in physical space.

Equations (22) describe a unique motion $y(x,t)$ and force $\sigma(t)$ in terms of x_0, x_1. To see it, combine (22b) and (22c) to give

$$W'(\lambda) = \sigma_{\max} - K\ell\lambda \quad \textit{add period} \tag{26}$$ eq:lamsol

In light of the assumed properties (8) of $W(\lambda)$, it is readily shown that there exists a unique root $\lambda > 0$ of this equation corresponding to any given $\ell > 0$, $K > 0$ and $\sigma_{\max}$. Moreover in view of (8f), the root λ decreases monotonically with increasing ℓ. The corresponding force is then given by (22b). These representations will of course involve given values of K, Y_0, Y_1 and the yet to be found values x_0, x_1.

The length ℓ of the body in reference space given through (22c) can be expressed in terms of force σ as

$$\ell = \bar{\ell}(\sigma) := \frac{\sigma_{\max} - \sigma}{K\widehat{\lambda}(\sigma)}, \tag{27}$$ eq:ls

for all $\sigma < \sigma_{\max}$, where the function $\widehat{\lambda}(\sigma)$ is the inverse of the force-stretch relation $\sigma = W'(\lambda)$ introduced in eq. (10). In view of (11)-(12), this shows that

$$\bar{\ell}\,'(\sigma) < 0, \quad \bar{\ell}(\sigma) \to +\infty \text{ as } \sigma \to -\infty, \quad \bar{\ell}(\sigma) \to 0^+ \text{ as } \sigma \to \sigma_{\max}^-. \tag{28}$$ eq:lsprop

The function $\bar{\sigma}(\ell)$ that is inverse to $\bar{\ell}(\sigma)$ obeys

$$\begin{aligned} &\bar{\ell}(\bar{\sigma}(\ell)) = \ell && \bar{\sigma}(\ell) \to \sigma_{\max}^- \quad \text{as} \quad \ell \to 0^+, \\ &\bar{\sigma}'(\ell) < 0 && \bar{\sigma}(\ell) \to -\infty \quad \text{as} \quad \ell \to +\infty\,. \end{aligned} \tag{29}$$ eq:sl

From equations (27)-(29) we can appreciate how growth, i.e. a change of the length of the bar ℓ in the reference configuration, affects force and stretch at equilibrium. A decrease in length ℓ in (27) produces an increase in stretch λ and in force σ till, eventually, ℓ goes to zero, stretch λ to infinity and the force to its maximum value $\sigma_{\max}$. Conversely, an increase in material length ℓ decreases both stretch and force. An indefinite increase of ℓ leads the force towards infinite compressive values and stretch towards zero.

I tried rephrasing this paragraph.

ss:DAEdiff

5.2. *Diffusion*

eq:dsol

The solution of the system of equations (3) yields

$$\begin{cases} \mu(y,t) = M_1 \dfrac{y - y_0}{y_1 - y_0} + \mu_0 \dfrac{y_1 - y}{y_1 - y_0}, & \forall\ y_0(t) \le y \le y_1(t) \qquad (30a) \quad \texttt{eq:dsol1} \\ h(y,t) = -m \dfrac{M_1 - \mu_0}{y_1 - y_0} \qquad (30b) \quad \texttt{eq:dsol2} \\ \mu_0 = M_1 + \dfrac{\varrho}{m}\,(y_1 - y_0)\,\dot{x}_0 \qquad (30c) \quad \texttt{eq:dsol3} \end{cases}$$

and we recall that $y_1 - y_0 = \lambda\ell$. Using (22c) and (25) one can express μ_0 in terms of the force σ,

$$\mu_0 = M_1 + \frac{\varrho}{Km}(\sigma_{\max} - \sigma)\,\dot{x}_0\,. \tag{31}$$ eq:mu0s

Observe that (31) can be used to eliminate the unknown chemical potential μ_0 from the other equations where its appears, namely (6a), (30a) and (30b).

Finally we note that if x_0 and x_1 are known, then as noted previously y_1 can be determined from (21), (25) and (26), $y_0 = Y_0$ being of course known. If in addition $\dot{x}_0$ is known then the chemical potential and flux fields are fully determined through (30).

ss:DAEaccr

5.3. Accretion

Using (31), setting $\mu_1 = M_1$ and noting that $\sigma_0(t) = \sigma_1(t) = \sigma(t)$, we rewrite the pair of kinetic equations (6) as

eq:asub

$$\begin{cases} \dot{x}_0(t) = -\dfrac{1}{B_0}\dfrac{\varrho(M_1 - M_{B,0}) + W^*(\sigma(t))}{1 + \frac{\varrho^2}{mB_0K}(\sigma_{\max} - \sigma)}, & \text{(32a)} \quad \texttt{eq:asub1} \\ \dot{x}_1(t) = \dfrac{1}{B_1}\left(\varrho(M_1 - M_{B,1}) + W^*(\sigma(t))\right) \quad \textit{add period} & \text{(32b)} \quad \texttt{eq:asub2} \end{cases}$$

We now introduce forces $\sigma_{\alpha 0}$, $\sigma_{\alpha 1}$ exploiting the bijectivity of $W^*(\sigma)$ in $\mathbb{R}$ at which the accretion rates $\dot{x}_0(t)$, $\dot{x}_1(t)$ vanish:

$$\sigma_{\alpha 0} \,:\, -W^*(\sigma_{\alpha 0}) = \varrho(M_1 - M_{B,0})\,, \quad \sigma_{\alpha 1} \,:\, -W^*(\sigma_{\alpha 1}) = \varrho(M_1 - M_{B,1})\,. \tag{33}$$ eq:salpha

Because of the monotonicity of W^* we see that $\sigma_{\alpha 0} < \sigma_{\alpha 1}$ if $M_{B,0} < M_{B,1}$ and vice versa. As to which of these holds will play a central role in Section 6.2 when we look at the existence of treadmilling states. Finally let the forces $\Delta\sigma$, σ_{asym} be defined by

$$\Delta\sigma \coloneqq \sigma_{\text{asym}} - \sigma_{\max} \coloneqq \frac{mB_0K}{\varrho^2} > 0\,. \tag{34}$$ eq:sasym

eq:afin

This allows us to write

$$\begin{cases} \dot{x}_0(t) = R_0(\sigma) \coloneqq -\dfrac{\Delta\sigma}{B_0}\,\dfrac{W^*(\sigma(t)) - W^*(\sigma_{\alpha 0})}{\sigma_{\text{asym}} - \sigma}, & \text{(35a)} \quad \texttt{eq:afin1} \\ \dot{x}_1(t) = R_1(\sigma) \coloneqq \dfrac{1}{B_1}\left(W^*(\sigma(t)) - W^*(\sigma_{\alpha 1})\right) \quad \textit{add comma} & \text{(35b)} \quad \texttt{eq:afin2} \end{cases}$$

for the accretion rates $\dot{x}_0(t)$, $\dot{x}_1(t)$ as functions $R_0(\sigma)$ and $R_1(\sigma)$ of the force, respectively.

Delete this next sentence since it was move above: Notice that $\sigma_{\alpha 0}$ and $\sigma_{\alpha 1}$ represent the values of force for which the accretion rates $\dot{x}_0(t)$, $\dot{x}_1(t)$ are zero. Since the chemical potential of the solvent bath M_1 can be varied, according to their definitions (33), the values of $\sigma_{\alpha 0}$ and $\sigma_{\alpha 1}$ may also be varied, but not independently. In addition, for the admissible values (24) of the force σ smaller than $\sigma_{\max}$, relation (34) and the monotonicity (14a) of $W^*(\sigma)$ tell us that

$$R_0(\sigma) \lesseqgtr 0 \;\text{ for } \sigma \gtreqless \sigma_{\alpha 0} \text{ and } \sigma < \sigma_{\max}\,, \quad R_1(\sigma) \gtreqless 0 \;\text{ for } \sigma \lesseqgtr \sigma_{\alpha 1}\,, \tag{36}$$ eq:R>0

underscoring in particular that $\sigma_{\alpha 0}$ and $\sigma_{\alpha 1}$ are the unique zeros of $R_0(\sigma)$ and $R_1(\sigma)$ respectively.

For $R_1(\sigma)$ we can easily infer its properties from those of W^*: it is a convex, monotonically increasing function whose image is all $\mathbb{R}$ and whose derivative tends to 0^+ for $\sigma \to -\infty$ and to $+\infty$ for $\sigma \to +\infty$.

Of $R_0(\sigma)$ we know that it tends to $-\infty$ as σ approaches σ_{asym} from below in the case where $\sigma_{\text{asym}} > \sigma_{\alpha 0}$. Using l'Hopital's rule we also deduce that $R_0(\sigma)$ tends to zero as $\sigma \to -\infty$. Looking at the first derivative of $R_0(\sigma)$,

$$R_0'(\sigma) = -\frac{\Delta\sigma}{B_0}\,\frac{W^*(\sigma) - W^*(\sigma_{\alpha 0}) + W^{*\prime}(\sigma)(\sigma_{\text{asym}} - \sigma)}{(\sigma_{\text{asym}} - \sigma)^2}\,, \tag{37}$$

eq:R0'

we observe that it is strictly negative for $\sigma_{\alpha 0} < \sigma < \sigma_{\text{asym}}$. Instead, R_0 is not monotonic for $\sigma < \sigma_{\alpha 0} < \sigma_{\text{asym}}$, since its derivative has opposite signs at the two ends of that interval.

ss:DAEeq

5.4. *Differential algebraic equation*

By (14a), (27) and (35) the model under consideration governing the evolution of the length ℓ of the bar in the reference configuration reduces to the following differential algebraic equation

eq:lsdae

$$\begin{cases} \dot\ell = R_1(\sigma) - R_0(\sigma) \\ \quad = \dfrac{1}{B_1}\,(W^*(\sigma) - W^*(\sigma_{\alpha 1})) + \dfrac{\Delta\sigma}{B_0}\,\dfrac{W^*(\sigma) - W^*(\sigma_{\alpha 0})}{\sigma_{\text{asym}} - \sigma}, & \text{(38a)} \quad \texttt{eq:lsdae1} \\ \ell = \bar\ell(\sigma) = \dfrac{\sigma_{\max} - \sigma}{K\ W^{*\prime}(\sigma)} \quad \textit{add comma} & \text{(38b)} \quad \texttt{eq:lsdae2} \end{cases}$$

in which $\ell(t)$ and $\sigma(t)$ are sought under initial conditions, see (7) and (25) ,

$$\ell(0) = x_{10} - x_{00}, \quad \sigma(0) = W'\left(\frac{Y_{10} - Y_0}{x_{10} - x_{00}}\right)\,, \tag{39}$$

eq:lsinit

and under the constraint $\ell > 0$ which is equivalent to $\sigma < \sigma_{\max}$.

sec:TM

6. Existence and stability of treadmilling solutions

In a so-called treadmilling solution the length $\ell = \ell_{\text{TM}}$ of the bar in the reference configuration does not vary with time: $\dot\ell = 0$, and this corresponds to values σ_{TM} of the force for which $R_0(\sigma_{\text{TM}}) = R_1(\sigma_{\text{TM}})$.

Moved text from here.

ss:TMstab

6.1. *Stability of treadmilling states*

We start by discussing the ~~condition of~~ stability of a treadmilling solution, assuming one to exist, by perturbing a treadmilling state characterized by force σ_{TM} and length $\ell_{\text{TM}} = \bar\ell(\sigma_{\text{TM}})$ according to (38b).

The perturbation of equation (10), $\lambda = \widehat{\lambda}(\sigma)$, yields

$$\delta\lambda = \widehat{\lambda}'(\sigma_{\rm TM})\delta\sigma \quad \textit{add period}$$

Operating analogously on equation (22c), $K\lambda\ell = \sigma_{\max} - \sigma$, gives

$$K\widehat{\lambda}(\sigma_{\rm TM})\delta\ell + K\ell_{\rm TM}\delta\lambda = -\delta\sigma \quad \textit{add period}$$

Combining the two preceding equations provides a relation between the perturbations $\delta\ell$ and $\delta\sigma$,

$$K\widehat{\lambda}(\sigma_{\rm TM})\,\delta\ell + \Big(K\ell_{\rm TM}\widehat{\lambda}'(\sigma_{\rm TM}) + 1\Big)\;\delta\sigma = 0. \tag{40}$$

eq:psell

From the expression (38a) of $\dot{\ell}(\sigma)$ we obtain

$$\delta\dot{\ell} = (R_1'(\sigma_{\rm TM}) - R_0'(\sigma_{\rm TM}))\;\delta\sigma.$$

Combining this with (40) yields

$$\delta\dot{\ell} = -F(\sigma_{\rm TM})\delta\ell \qquad \text{where} \quad F(\sigma_{\rm TM}) = \frac{R_1'(\sigma_{\rm TM}) - R_0'(\sigma_{\rm TM})}{K\ell_{\rm TM}\widehat{\lambda}'(\sigma_{\rm TM}) + 1}\,K\widehat{\lambda}(\sigma_{\rm TM}).$$

The treadmilling solution is stable if the linear ordinary differential equation $\delta\dot{\ell}(t) = -F(\sigma_{\rm TM})\delta\ell(t)$ has exponentially decaying solutions[1], and this occurs if and only if $F(\sigma_{\rm TM}) > 0$. Since $\widehat{\lambda}(\sigma_{\rm TM}) > 0$, $\ell_{\rm TM} > 0$ and $\widehat{\lambda}'(\sigma_{\rm TM}) > 0$ it follows that the treadmilling solution is stable if and only if

$$R_1'(\sigma_{\rm TM}) > R_0'(\sigma_{\rm TM}). \tag{41}$$

eq:TMstable

It is interesting to use the monotonic relation ~~(27)~~ between the force σ and the referential length ℓ to plot the evolution of the system in the neighborhood of a stable treadmilling solution on the $\ell, \dot{\ell}$-plane. The system (38) can be written using (29) as $\dot{\ell} = R_1(\bar{\sigma}(\ell)) - R_0(\bar{\sigma}(\ell))$. Given that $\bar{\sigma}(\ell)$ is a monotonically decreasing function, the slope of $\dot{\ell}(\ell)$ is thus seen to be negative close to a stable treadmilling in view of (41).

This is shown schematically in Figure 3. Observe how, if $\ell > \ell_{\rm TM}$ at some time then $\dot{\ell} < 0$ and so $\ell(t)$ will decrease until it reaches the treadmilling value $\ell_{\rm TM}$. Likewise if $\ell < \ell_{\rm TM}$, $\ell(t)$ will increase to $\ell_{\rm TM}$.

ss:TMexist

6.2. *Existence of treadmilling solutions*

Suppose that in the limit $\ell \to 0$, i.e. $\sigma \to \sigma_{\max}$, accretion prevails over ablation in the sense that $\dot{\ell} > 0$. By (38a) this is equivalent to

$$R_1(\sigma_{\max}) > R_0(\sigma_{\max})\,. \tag{42}$$

eq:R1>R0

[1] If $\delta\ell(t)$ vanishes exponentially then so do the perturbations of the various other quantities.

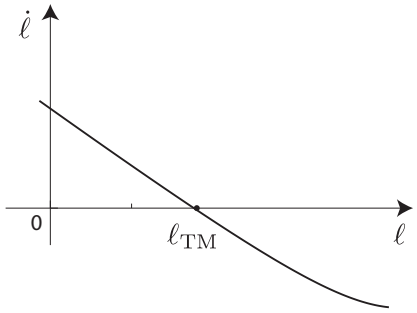

Figure 3: Graph of $\dot{\ell} = \dot{x}_1 - \dot{x}_0 = R_1(\bar{\sigma}(\ell)) - R_0(\bar{\sigma}(\ell))$ versus ℓ where $\bar{\sigma}(\ell)$ is given through (29). Figure caption has been edited. Bars over sigmas and eqn number. fig:ell

It is possible to formulate (42) in a more convenient form by introducing the force σ_β according to

$$W^*(\sigma_\beta) = \frac{1}{1+\beta} W^*(\sigma_{\alpha 0}) + \frac{\beta}{1+\beta} W^*(\sigma_{\alpha 1}) \,, \quad \text{with} \quad \beta = \frac{B_0}{B_1} > 0 \,. \tag{43}$$ eq:sb

From the monotonicity of W^*, it is clear that the value of σ_β always lies between $\sigma_{\alpha 0}$ and $\sigma_{\alpha 1}$ defined in (33). It is readily seen that the inequality (42) is equivalent to

$$\sigma_\beta < \sigma_{\rm max} \,. \tag{44}$$ eq:sb<smax

The inequality (44), i.e. the condition that accretion prevails over ablation in the limit $\ell \to 0$, will play a central role in the results to follow.

sss:TM0<1

6.2.1. Case $M_{B,0}$ smaller than $M_{B,1}$:

We discuss first the case that is more relevant with regard to ~~the~~ applications (**??**) and experiments (**????**) where the treadmilling state involves accretion at the fixed end Y_0 and ablation at the free end y_1 (rather than the converse).

Suppose that

$$M_{B,0} < M_{B,1} \quad \textit{add comma} \tag{45}$$ eq:MB0<MB1

corresponding to the actin being in its ATP form at Y_0 and the hydrolyzed ADP form at y_1. From the definition (33) and ~~from~~ the monotonicity (14a) of W^*, it follows that (45) holds if and only if

$$\sigma_{\alpha 0} < \sigma_{\alpha 1} \,. \tag{46}$$ eq:sa0<sa1

Under the above provision, it is possible to prove that,

prop-1

Proposition 1 (Existence and uniqueness)**.** *Given that* (45) *(equivalently* (46)*) holds, $\sigma_\beta < \sigma_{\rm max}$ is a necessary and sufficient condition for the existence and uniqueness of a treadmilling solution. Such a solution is globally stable.*

Proof. To show sufficiency, assume $\sigma_\beta < \sigma_{\max}$ holds. Since σ_β lies between $\sigma_{\alpha 0}$ and $\sigma_{\alpha 1}$ it now follows that in the present case

$$\sigma_{\alpha 0} < \sigma_\beta < \sigma_{\max} < \sigma_{\text{asym}}. \tag{47}$$

eq:stressineq

Deleted sentence. Moreover, as observed in section 5.3, in the interval $\sigma_{\alpha 0} < \sigma < \sigma_{\max}$

- $R_0(\sigma)$ is negative,
- $R_0(\sigma)$ is monotonically decreasing,
- $R_1(\sigma)$ is monotonically increasing,
- $R_1(\sigma_{\alpha 0}) < R_0(\sigma_{\alpha 0}) = 0$,
- $R_1(\sigma_{\max}) > R_0(\sigma_{\max})$.

Given the continuity of $R_0(\sigma)$ and $R_1(\sigma)$, and because their difference has opposite signs at the extremes of the interval, it follows that they have the same value at some $\sigma = \sigma_{\text{TM}}$ in this interval. Uniqueness follows from monotonicity. The negative sign of $R_0(\sigma_{\text{TM}})$ implies that R_1 too is negative at σ_{TM}, and therefore the treadmilling force lies in the interval $\sigma_{\alpha 0} < \sigma_{\text{TM}} < \min(\sigma_{\alpha 1}, \sigma_{\max})$. Moreover, since $\dot{x}_0 = \dot{x}_1 = R_0(\sigma_{\text{TM}}) = R_1(\sigma_{\text{TM}}) < 0$ at treadmilling, accretion takes place at Y_0 and ablation at y_1. From monotonicity we also additionally infer that condition (41) is met and that the unique treadmilling solution is always stable. In fact it is globally stable because the rate $\dot{\ell} = R_1(\sigma) - R_0(\sigma)$ is always negative for all $\sigma < \sigma_{\text{TM}}$, i.e. for $\ell > \ell_{\text{TM}}$, and vice versa $\dot{\ell} > 0$ for $\sigma_{\text{TM}} < \sigma < \sigma_{\max}$.

To show necessity, assume conversely that $\sigma_\beta \geq \sigma_{\max}$. The case $\sigma_\beta = \sigma_{\max}$ corresponds to a non admissible treadmilling solution in which the bar has zero reference length ℓ and force equal to $\sigma_{\max}$. Can you help the reader (and me) by pointing to some equations that show this to be the case?

Turning to the case $\sigma_\beta > \sigma_{\max}$, first consider the subcase where $\sigma_{\alpha 0} \geq \sigma_{\max}$. According to (36), there is no intersection in the interval $\sigma < \min(\sigma_{\alpha 0}, \sigma_{\max}) < \sigma_{\alpha 1}$, because $R_0(\sigma)$ is positive and $R_1(\sigma)$ negative. This ends the proof for this subcase. If $\sigma_{\alpha 0} < \sigma_{\max}$, we consider the interval $\sigma_{\alpha 0} \leq \sigma < \sigma_{\max}$: both $R_0(\sigma)$ and $R_1(\sigma)$ are monotonic and R_0 is above R_1 at both ends of the interval. Hence any intersection is excluded also in this case.

□

An example of functions R_0 and R_1 in the case $\sigma_{\alpha 0} < \sigma_{\alpha 1}$ is shown in Figure 4. There we see that at $\sigma = \sigma_{\max}$, condition (42), is met and therefore a unique, globally stable, treadmilling solution exists. This result corroborates the globally stable equilibrium observed numerically by **?** in a similar setting.

Once the value of the force σ_{TM} at treadmilling is known, it is possible to reconstruct the whole system at treadmilling. The corresponding stretch λ_{TM} is given by $\lambda_{\text{TM}} = \widehat{\lambda}(\sigma_{\text{TM}})$; the growth rates at the two ends are $\dot{x}_0^{\text{TM}} = \dot{x}_1^{\text{TM}} = R_0(\sigma_{\text{TM}}) = R_1(\sigma_{\text{TM}})$; the length of the body in reference space is $\ell_{\text{TM}} = \bar{\ell}(\sigma_{\text{TM}})$;

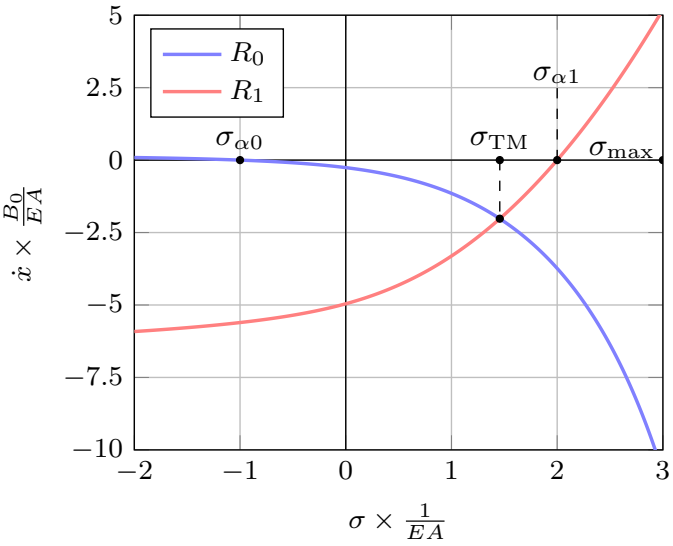

Figure 4: Example of treadmilling solution obtained using $W^*(\sigma)$ from eq. (16) with parameters $\sigma_{\mathrm{asym}} = 5EA$, $\sigma_{\max} = 3EA$, $\sigma_{\alpha 0} = -EA$, $\sigma_{\alpha 1} = 2EA$, $\beta = 1.0$.Can you move the $\sigma_{\max}$ to the right of the box or place it right above the black dot?

fig:tm1

the length of the body in physical space is $\lambda_{\mathrm{TM}}\ell_{\mathrm{TM}}$; and the chemical potential at the growing end is $\mu_0^{\mathrm{TM}} = M_1 + \varrho(\sigma_{\max} - \sigma_{\mathrm{TM}})\dot{x}_0^{\mathrm{TM}}/(Km)$.

If (46) holds but (44) does not, then differently from the situation represented in Figure 4, the value of $\sigma_{\max}$ is smaller than σ_{TM}, the point where R_0 and R_1 intersect, and so there is no treadmilling solution. According to (38a), we have $\dot{\ell}$ negative everywhere in the admissible domain, so if the bar has some nonzero length at the initial instant, the it progressively loses all of its monomers till it reaches $\ell = 0$ and $\sigma = \sigma_{\max}$.

It is interesting to represent the evolution in space (Figure 5) and time (Figure 6) of the energy of a material unit of actin as it undergoes treadmilling.

The energy e of a material unit is comprised of its chemical potential μ, elastic strain energy W and the potential energy of the stress $\sigma\lambda$: $e = \rho\mu + W - \sigma\lambda = \rho\mu - W^*$. In Figures 5 and 6 the points (f) and (a) correspond to states just before and after accretion, while (d) and (e) refer to just before and after ablation. The energy of a free monomer at Y_0, just before accretion, is $e_f = \rho\mu_0$, and just after accretion, when it is bound to the solid, its energy is $e_a = \rho M_{B,0} - W^*(\sigma_0)$. The difference between these two energies is precisely the driving force at Y_0: $F_0 = e_f - e_a$. The dissipation inequality requires $F_0 V_0 = -F_0\dot{x}_0 \geq 0$. When accretion takes place $\dot{x}_0 < 0$ and therefore $F_0 \geq 0$ or equivalently $e_a \leq e_f$. Likewise the energy of a material unit at y_1, when it is still bound to the solid, is $e_d = \rho M_{B,1} - W^*(\sigma_1)$ and when it is free after ablation it is $e_e = \rho\mu_1$. The corresponding driving force is $F_1 = e_e - e_d$ and the

dissipation inequality requires $F_1 V_1 = F_1 \dot{x}_1 \geq 0$. When ablation takes place at y_1, $\dot{x}_1 < 0$ and so $F_1 \leq 0$ and $e_e \leq e_d$.

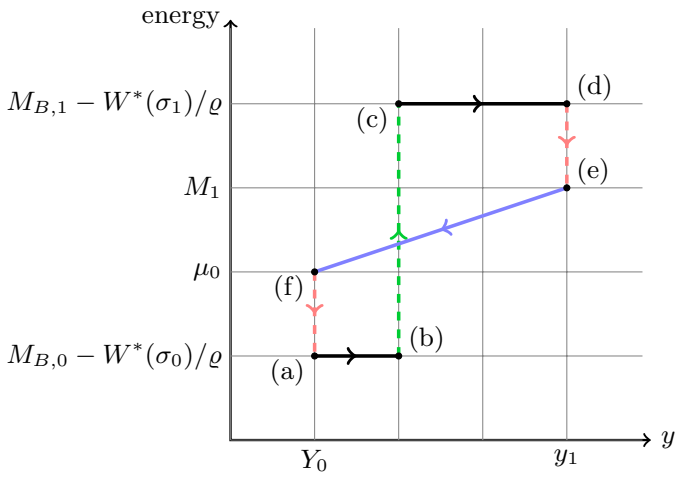

Figure 5: Evolution in space of the energy of a mole of actin as it undergoes treadmilling. Blue represents diffusion, red accretion/ablation and green ATP-hydrolysis.

fig:tm-eny

A unit of ATP-actin when it is a free monomer in the monomer pool and is located at the right-hand end of the bar corresponds to point (e) in Figure 5. As it diffuses through the bar it goes from $(e) \to (f)$ following the blue path, and eventually arrives at the left-hand end of the bar. Accretion then takes place as described in the preceding paragraph and the material unit follows the path $(f) \to (a)$ following the red dashed line, losing energy in the process. The actin unit that got attached to the solid at (a) is now progressively pushed outwards along the bar (due to the accretion of additional material at the left end) and moves towards the right-hand end. This corresponds to $(a) \to (b) \to (c) \to (d)$ with the green segment $(b) \to (c)$ being associated with the hydrolysis step where ATP is converted to ADP which has a higher chemical potential. The location along the bar at which hydrolysis takes place is not determined in our model. Once this ADP-unit reaches the right-hand end at (d) it undergoes ablation and is detached from the solid following the red dashed line accompanied by an energy loss. It has now returned to the starting point (e) and the process starts again (Eric question: when does ADP actin becomes ATP actin again? and is there an energy jump in the process?). The same evolution is represented in Figure 6, with the difference that, consistently with the model assumptions, the Rohan: I guess this is correct since we effectively take the diffusion coefficient to be infinite in the diffusion equation. And yet there is a speed associated with monomer diffusion mM_1/ρ and speeds associated with kinetics $\rho M_1/B$ and we do not mean that the former is much greater than the latter. instantaneous diffusion segment is vertical.

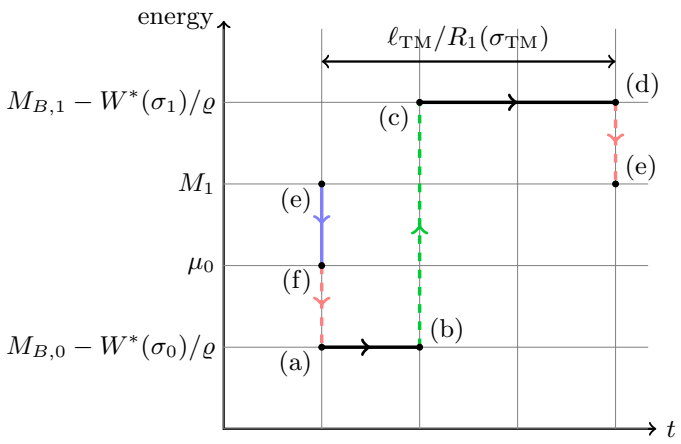

Figure 6: Evolution in time of the energy of a mole of actin as it undergoes treadmilling. Blue represents diffusion, red accretion/ablation and green ATP-hydrolysis. fig:tment

sss:TM0>1

6.2.2. Case $M_{B,0}$ larger than $M_{B,1}$.

We now discuss the case in which at treadmilling accretion takes place at the free end y_1, and ablation at the fixed end Y_0. This situation could resemble the experimental set-ups of **?** and **?**, though treadmilling was not investigated there.

Suppose that

$$M_{B,0} > M_{B,1}, \tag{48}$$

eq:MB0>MB1

that is, actin is in its ATP form at y_1 and the hydrolyzed ADP form at Y_0. From the definition (33) and from the monotonicity (14a) of W^*, it follows that (48) holds if and only if

$$\sigma_{\alpha 0} > \sigma_{\alpha 1} \quad \textit{add period.} \tag{49}$$

eq:sa0>sa1

Under the above condition, it is possible to prove that,

prop-2

Proposition 2 (Existence)**.** *Given that (48) (equivalently (49)) holds, $\sigma_\beta < \sigma_{\max}$ is a sufficient condition for the existence of a treadmilling solution.*

Proof. Assume that $\sigma_\beta < \sigma_{\max}$ holds. Then since $\sigma_{\alpha 1} < \sigma_\beta < \sigma_{\alpha 0}$ it follows that $\sigma_{\alpha 1} < \sigma_{\max}$. Moreover, as observed in section 5.3, in the interval $\sigma_{\alpha 1} < \sigma < \sigma_{\max}$

- $R_1(\sigma)$ is positive,
- $R_0(\sigma_{\alpha 1}) > 0 = R_1(\sigma_{\alpha 1})$ since $\sigma_{\alpha 1} < \sigma_{\alpha 0}$, and
- $R_1(\sigma_{\max}) > R_0(\sigma_{\max})$ by (42) and (44).

Given the continuity of $R_0(\sigma)$ and $R_1(\sigma)$, the two functions certainly intersect at least once between $\sigma_{\alpha 1}$ and $\sigma_{\max}$ because their difference has opposite signs at the extremes of the interval. Positiveness of $R_1(\sigma)$, implies that both $R_0(\sigma_{\rm TM})$ and $R_1(\sigma_{\rm TM})$ are positive, and so $\dot{x}_0 = \dot{x}_1 > 0$ corresponding to ablation at Y_0 and accretion at y_1. Such a treadmilling state may only exist in the interval $\sigma_{\alpha 1} < \sigma_{\rm TM} < \min(\sigma_{\alpha 0}, \sigma_{\max})$. The solution need not be unique because R_0 is not necessarily monotonic for $\sigma < \sigma_{\alpha 0}$.

□

An example of functions R_0 and R_1 in the case $\sigma_{\alpha 0} > \sigma_{\alpha 1}$ is shown in Figure 7. The figure has been drawn for a case in which $\sigma_{\rm asym} < \sigma_{\alpha 0}$ and in

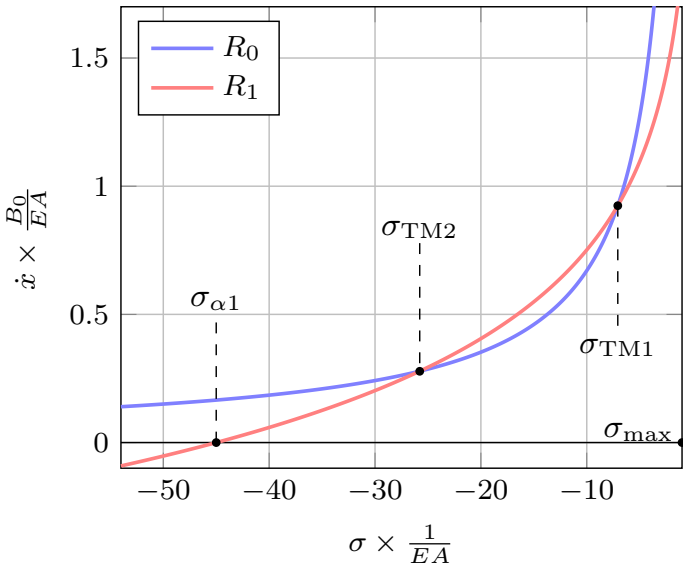

Figure 7: Example of treadmilling solution obtained using $W^*(\sigma)$ from eq. (16) with parameters $\sigma_{\rm asym} = 0$, $\sigma_{\max} = -EA$, $\sigma_{\alpha 0} = 2EA$, $\sigma_{\alpha 1} = -45EA$, $\beta = 1.0$. (I haven't so far been able to find multiple intersections in the case $\sigma_{\alpha 0} < \sigma_{\rm asym}$)

fig:tm2

which, correspondingly, both R_0 and R_1 are monotonically increasing in the domain $\sigma < \sigma_{\max}$. Notice that multiple treadmilling solutions exist despite conditions (42), (44) not being met, because in the current case, $\sigma_{\alpha 1} < \sigma_{\alpha 0}$, such conditions are sufficient but not necessary for the existence of treadmilling solutions. According to the local stability criterion (41), the ~~first~~ treadmilling state characterized by force $\sigma_{\rm TM1}$ is unstable while the other at force $\sigma_{\rm TM2}$ is stable. The basin of attraction of the latter solution is any initial condition corresponding to a force $\sigma < \sigma_{\rm TM1}$. A bar whose initial length $\ell(0) < \ell_{\rm TM1}$, i.e. $\sigma(0) > \sigma_{\rm TM1}$, will have negative $\dot{\ell}(t)$ and therefore progressively lose all of its monomers and approach zero length and force $\sigma_{\max}$.

sec:end

7. Conclusions

In the study we have formulated and analyzed a one-dimensional, self-contained growth model for an actin bar fixed at one end and elastically constrained at the other. The model encompasses diffusion in a solvent surrounding or permeating the bar as well as growth conditions at the ends. The nonlinear elastic properties of actin are specified through an arbitrary convex strain energy density function.

Treadmilling states were investigated in which the length of the bar remains constant while accreting actin monomers at one end and ablating them at the opposite end at equal rates. The treadmilling state in which monomers accrete at the fixed end is found to be globally stable. Multiple treadmilling states in which monomers ablate at the fixed end are instead possible.

Conditions for existence and stability of treadmilling states were condensed into relatively simple formulas, (44), (45) and (48), which are useful in understanding the influence of the different parameters of the model, and may help explain the results of more complex models. For instance, global stability of treamilling states accreting monomers at the fixed end can provide additional explanation to the numerical findings made by **?** in a similar setting.

It is illuminating to interpret the main results of this study, Propositions 1 and 2, in terms of the chemical potential M_1 of free monomers and the referential length ℓ of the bar. In a laboratory experiment one can imagine varying M_1 and observing how ℓ changes.

First consider how each end of the bar grows in different regions of the ℓ, M_1-plane. The curves $\mathcal{C}_0$ and $\mathcal{C}_1$ at which $V_0 = 0$ and $V_1 = 0$ are shown in Figure 8 in the **case** $M_{B,1} > M_{B,0}$ (the case of principal interest). By (32) and (29) they are characterized by

$$\mathcal{C}_0 : \ M_1 = M_{B,0} - W^*(\overline{\sigma}(\ell))/\varrho, \qquad \mathcal{C}_1 : \ M_1 = M_{B,1} - W^*(\overline{\sigma}(\ell))/\varrho. \tag{50}$$

eq:0502-eq4

That these curves have the monotonicity depicted in the figure follows from the properties of $\overline{\sigma}(\ell)$ and $W^*(\sigma)$ which tell us that $-W^*(\overline{\sigma}(\ell))$ increases monotonically from $W^*(\sigma_{\max})$ to $+\infty$ as ℓ increases from $\ell = 0$. These curves demarcate 3 regions of the ℓ, M_1-plane where the signs of the growth velocities $V_0 = -\dot{x}_0$ and $V_1 = \dot{x}_1$ are as shown. Observe that if the bar is sufficiently long or the chemical potential is sufficiently small, corresponding to points on the right of $\mathcal{C}_0$, ablation happens at both ends of the bar ($V_1 < 0, V_0 < 0$) and it will grow shorter. On the other hand on the left of $\mathcal{C}_1$, where the bar is sufficiently short or the chemical potential is sufficiently large, accretion happens at both ends ($V_1 > 0, V_0 > 0$) and the bar will grow longer. Between the two curves $\mathcal{C}_0$ and $\mathcal{C}_1$, where the length ℓ of the bar and the chemical potential M_1 have intermediate values, accretion occurs at the left-hand end ($V_0 > 0$) and ablation occurs at the right-hand end ($V_1 < 0$).

The curve $\mathcal{C}_{TM}$ corresponding to treadmilling is found by setting $V_0 =$

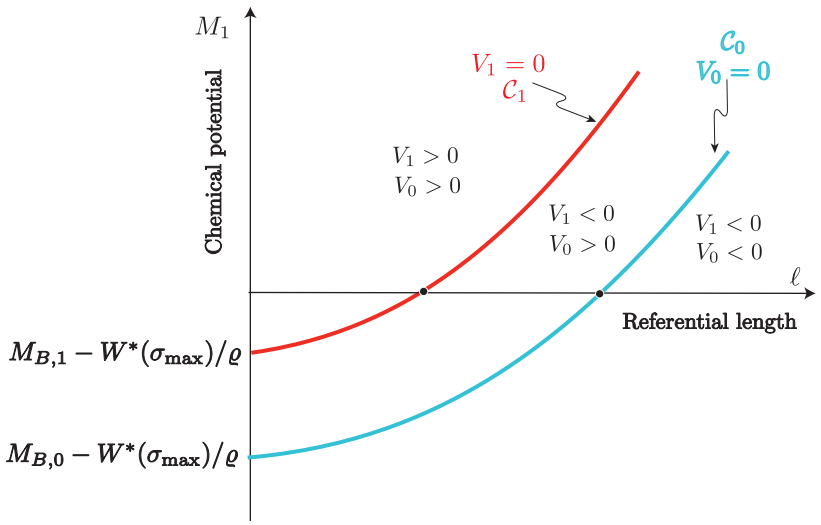

Figure 8: The ℓ, M_1-plane in the case $M_{B,1} > M_{B,0}$. The growth rates V_0 and V_1 vanish on the respective curves $\mathcal{C}_0$ and $\mathcal{C}_1$. These curves demarcate 3 regions of the ℓ, M_1-plane where the signs of the growth velocities are as shown. Accretion happens at both ends of the bar to the left of $\mathcal{C}_1$ (i.e. large M_1 and small ℓ) while abbation occurs at both ends of the bar to the right of $\mathcal{C}_0$ (i.e. small M_1 and large ℓ). Between these curves accretion occurs at x_0 while ablation occurs at x_1. Contrast this with Figure 10. Fig-x0x1a

$-V_1 \,(\neq 0)$, i.e. $\dot{x}_0 = \dot{x}_1$, which from (32) is found to be described by

$$\mathcal{C}_{TM}: \; M_1 = \overline{M}_1(\ell) := \frac{M_{B,0} + \beta\left[1 + \frac{\rho^2}{mB_0K}(\sigma_{\max} - \overline{\sigma}(\ell))\right] M_{B,1}}{1 + \beta\left[1 + \frac{\rho^2}{mB_0K}(\sigma_{\max} - \overline{\sigma}(\ell))\right]} - W^*(\overline{\sigma}(\ell))/\varrho. \tag{51}$$

eq:0502-eq2

It is clear from (50) and (51) that $\mathcal{C}_{TM}$ necessarily lies between the two curves $\mathcal{C}_0$ and $\mathcal{C}_1$ as shown in Figure 9. The monotonicity of $\mathcal{C}_{TM}$ depicted in the figure follows from the existence of unique treadmilling states corresponding (in particular) to all values of the chemical potential M_1 for which equation (53) below holds (Proposition 1). By setting $\ell = 0$ in (51) we see that $\mathcal{C}_{TM}$ cuts the M_1-axis at

$$M_1 = \overline{M}_1(0) = \frac{M_{B,0} + \beta M_{B,1}}{1 + \beta} - W^*(\sigma_{\max})/\varrho. \tag{52}$$

eq:0503-eq1

It follows that, corresponding to any given value of the chemical potential

$$M_1 > \overline{M}_1(0) = \frac{M_{B,0} + \beta M_{B,1}}{1 + \beta} - W^*(\sigma_{\max})/\varrho, \tag{53}$$

eq:0502-eq1

there is a corresponding length of the bar $\ell = \ell_{TM} > 0$ such that (ℓ_{TM}, M_1) lies on $\mathcal{C}_{TM}$, or stated differently, a unique treadmilling solution exists whenever (53) holds. It is not difficult to show that the inequality (53) is equivalent to the inequality (44) (which in turn is equivalent to (42)).

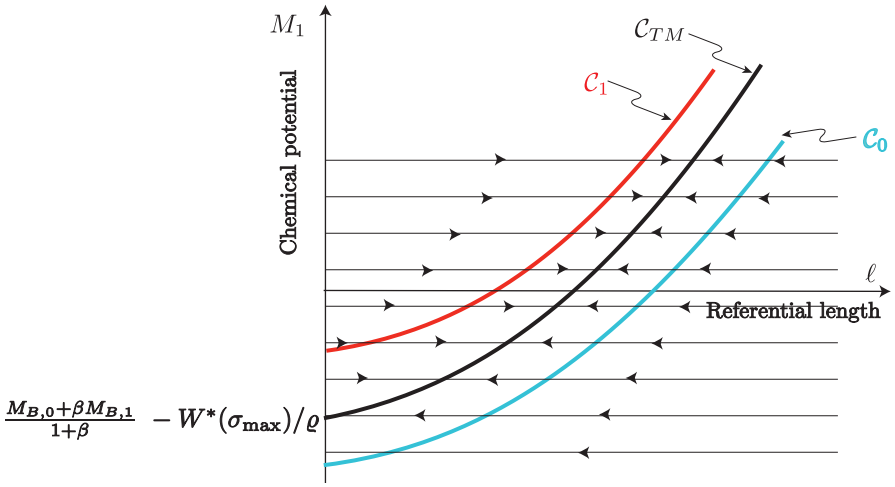

Figure 9: A point (ℓ, M_1) on the curve $\mathcal{C}_{TM}$ corresponds to a treadmilling state. The arrow at an arbitrary point (ℓ, M_1) tells us whether $\dot{\ell}$ is positive or negative there thus indicating whether the length of the bar increases or decreases. Observe from the figure that a treadmilling solution exists whenever (53) holds.

Fig-x0x1b

The value of $\dot{\ell}$ corresponding to each point (ℓ, M_1) of the ℓ, M_1-plane can be calculated using (38a) and $\sigma = \overline{\sigma}(\ell)$ from (29). The arrows in Figure 9 indicate whether this value of $\dot{\ell}$ is positive or negative. If M_1 is held constant (as we have done) then the system starting out initially at some point of the ℓ, M_1-plane will follow the $M_1 =$ constant line through that point in the direction indicated by the arrows. The stability of the treadmilling solution is evident.

If the chemical potential of the free monomers does not obey (53), i.e. if

$$M_1 < \overline{M}_1(0) = \frac{M_{B,0} + \beta M_{B,1}}{1+\beta} - W^*(\sigma_{\max})/\varrho, \tag{54}$$

we see from Figure 9 that (a) there is no corresponding treadmilling state, and (b) if the bar has some positive length at the initial instant, it will mononotically get shorter and eventually disappear.

Now consider the **case** $M_{B,1} < M_{B,0}$. Figure 10 shows the ℓ, M_1-plane and the signs of the growth velocities on different regions of it. The treadmilling curve, still characterized by (51), has the properties that (a) it lies between $\mathcal{C}_0$ and $\mathcal{C}_1$, (b) it passes through $(0, \overline{M}_1(0))$ where $\overline{M}_1(0)$ continues to be given by (52), and (c) $\overline{M}_1(\ell) \to \infty$ as $\ell \to \infty$. Thus it is clear that there necessarily exists a treadmilling solution corresponding to any $M_1 > \overline{M}_1(0)$ which illustrates the result in Proposition 2. However the curve $\mathcal{C}_{TM}$ is not necessarily monotonically rising and so (i) there may exist multiple treadmiling states corresponding to a given value of M_1 and (ii) there may exist treadmiling states for values of M_1 in the range $M_{B,1} - W^*(\sigma_{\max})/\varrho < M_1 < \overline{M}_1(0)$. Note from Figure 10 that, since the treadmilling curve lies between $\mathcal{C}_0$ and $\mathcal{C}_1$, all such solutions involve

accretion at the right-hand end and ablation at the left-hand (in contrast to the case $M_{B,1} > M_{B,0}$ shown in Figure 8.

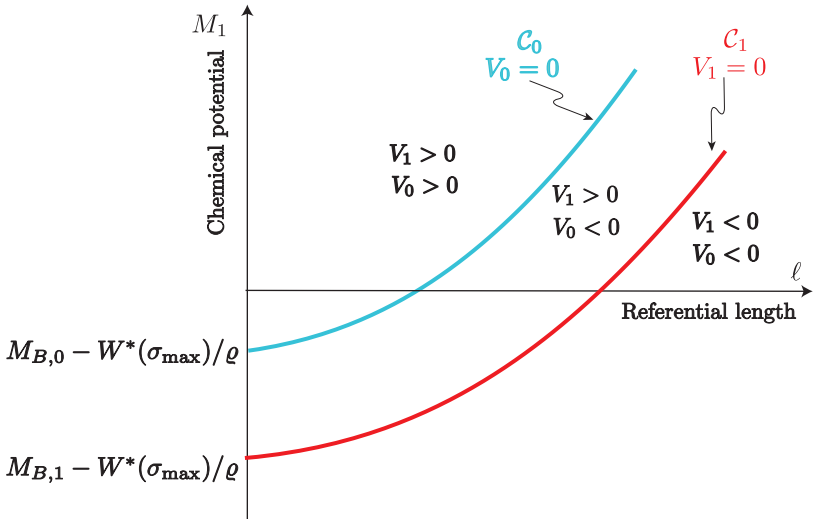

Figure 10: The ℓ, M_1-plane in the case $M_{B,1} < M_{B,0}$. The growth rates V_0 and V_1 vanish on the respective curves $\mathcal{C}_0$ and $\mathcal{C}_1$. Accretion happens at both ends of the bar to the left of $\mathcal{C}_0$ (i.e. large M_1 and small ℓ) while abbation occurs at both ends of the bar to the right of $\mathcal{C}_1$ (i.e. small M_1 and large ℓ). Between these curves accretion occurs at x_1 while ablation occurs at x_0. Contrast this with Figure 8. The treadmilling curve $\mathcal{C}_{TM}$, not shown, is a not-necessarily monotonic curve that lies between $\mathcal{C}_0$ and $\mathcal{C}_1$. See text for more information. Fig-x0x1c

Further refinements of the model would ~~also~~ be relevant for applications, especially experimental ones: accounting for the density and see earlier comments on stiffness. stiffness increase of actin under higher external load and developing analytical relationships between growth velocity and applied force are two of them. Finally, extension of the present work to the stability of two dimensional treadmilling states previously studied in **?** is planned.

Acknowledgements

R.A. and E.P. gratefully acknowledge the support of the MIT-FVG Seed Fund. E.P. thankfully acknowledges as well the support of the Italian National Group of Mathematical Physics (GNFM-INdAM).

Other errors: Parekh et al 2005 paper is December (not November) and page numbers are 1119-1129.

There were some strange symbols in bibtex for the Chaudhuri 2007 reference that I cleaned up.